TOR complex 2–Ypk1 signaling regulates actin polarization via reactive oxygen species

Brad J. Niles and Ted Powers
Department of Molecular and Cellular Biology, College of Biological Sciences, University of California, Davis, Davis, CA 95616

ABSTRACT The evolutionarily conserved mTOR complex 2 (mTORC2) signaling pathway is an important regulator of actin cytoskeletal architecture and, as such, is a candidate target for preventing cancer cell motility and invasion. Remarkably, the precise mechanism(s) by which mTORC2 regulates the actin cytoskeleton have remained elusive. Here we show that in budding yeast, TORC2 and its downstream kinase Ypk1 regulate actin polarization by controlling reactive oxygen species (ROS) accumulation. Specifically, we find that TORC2-Ypk1 regulates actin polarization both by vacuole-related ROS, controlled by the phospholipid flippase kinase Fpk1 and sphingolipids, and by mitochondria-mediated ROS, controlled by the PKA subunit Tpk3. In addition, we find that the protein kinase C (Pkc1)/MAPK cascade, a well-established regulator of actin, acts downstream of Ypk1 to regulate ROS, in part by promoting degradation of the oxidative stress responsive repressor, cyclin C. Furthermore, we show that Ypk1 regulates Pkc1 activity through proper localization of Rom2 at the plasma membrane, which is also dependent on Fpk1 and sphingolipids. Together these findings demonstrate important links between TORC2/Ypk1 signaling, Fpk1, sphingolipids, Pkc1, and ROS as regulators of actin and suggest that ROS may play an important role in mTORC2-dependent dysregulation of the actin cytoskeleton in cancer cells.

INTRODUCTION

For cells to adapt to changing conditions, they must be able to respond rapidly to intracellular and environmental cues. Remodeling of the actin cytoskeleton is one method cells use to accomplish this, and its importance is highlighted by its involvement in a number of physiological processes, including cell growth and division, chemotaxis, and neurite extension, as well as in polarized growth in budding yeast (Mammoto and Ingber, 2009; Mooren et al., 2012; Taulet et al., 2012). There are a number of molecules that regulate actin cytoskeletal architecture, including actin-binding proteins such as profilin, the G-proteins Rac and Rho, and mitogen-activated protein kinase (MAPK) signaling cascades, as well as a recently emerging

role for reactive oxygen species (ROS; Fiaschi et al., 2006; Moseley and Goode, 2006). A balance of ROS and antioxidant defense systems allows actin to alternate between oxidized and reduced forms, with reactions centered at two highly conserved redox-sensitive cysteine (Cys) amino acid residues, Cys-272 and Cys-374. Oxidation of these residues leads to formation of a disulfide bridge and actin dimers, which can positively affect certain cellular functions, such as motility (Lassing et al., 2007; Taulet et al., 2012). However, defects in the regulation of ROS in conditions such as sickle cell disease lead to actin oxidation and an altered actin cytoskeleton in sickled red blood cells (Shartava et al., 1995). In addition, ROS have been implicated in tumor cell migration and invasion, through regulation of the actin cytoskeleton (Park et al., 2012). Thus determining how ROS is regulated in cells is important for understanding conditions that lead to defects in actin cytoskeletal architecture.

We recently demonstrated that an important regulator of ROS is target of rapamycin complex 2 (TORC2), an evolutionarily conserved regulator of cell growth in eukaryotic organisms (Niles et al., 2014). We observed that TORC2, through its downstream target kinase Ypk1, regulates ROS produced from both mitochondrial and nonmitochondrial sources, including changes in acidification of the vacuole. We demonstrated that maintenance of vacuolar acidification by TORC2/Ypk1 signaling requires both proper levels of sphingolipids

and regulation of the phospholipid flippase kinase Fpk1 (Niles *et al.*, 2014). A well-characterized phenotype of TORC2 mutants is dysregulation of actin, establishing TORC2 as a promoter of actin polarization in both mammalian and yeast cells (Helliwell *et al.*, 1998a; Jacinto *et al.*, 2004). In yeast, actin is organized into actin cables and cortical actin patches, where patches are normally clustered within the emerging bud tip, and is essential for daughter cell formation (Moseley and Goode, 2006). TORC2-dependent regulation of the actin cytoskeleton is required to maintain the polarized nature of cell growth in budding yeast and is required for endocytosis as well as genome stability in response to DNA damage (deHart *et al.*, 2003; Shimada *et al.*, 2013). However, the mechanism by which TORC2 signaling regulates the actin cytoskeleton remains poorly understood.

In mammalian cells, mTORC2 phosphorylation of protein kinase C α (PKCα) and PKCζ is required for proper actin cytoskeletal organization and migration (Ikenoue *et al.*, 2008; Li and Gao, 2014). Similarly, Pkc1 in yeast is known to play a role in the regulation of actin downstream of TORC2, as overexpression of an activated allele of Pkc1 (Pkc1^{R398P}) rescues the actin depolarization phenotype of *torc2* and *ypk1Δ* mutants (Helliwell *et al.*, 1998b; Roelants *et al.*, 2002; Schmelzle *et al.*, 2002). However, direct regulation of Pkc1 by TORC2 has not been observed in yeast. Instead, Pkc1 is activated by the GTPase Rho1, which is itself regulated by a balance of GTPase-activating proteins (GAPs) and guanine nucleotide exchange factors (GEFs; Bickle *et al.*, 1998; Nonaka *et al.*, 1995). Whereas overexpression of the GEF Rom2 also rescues the growth and actin defects of TORC2 mutants (Schmidt *et al.*, 1997), links between TORC2 or its downstream target kinase Ypk1 and Rom2/Rho1 and Pkc1/MAPK signaling have not been identified. Here we address this issue and identify a number of important functional interactions by which TORC2/Ypk1 signaling regulates actin polarization via modulation of ROS, including interactions between Fpk1, sphingolipids, and Pkc1/MAPK activity.

RESULTS

Ypk1-dependent ROS perturbs actin cytoskeleton organization

In a previous study, we demonstrated that TORC2-Ypk1 signaling suppresses ROS accumulation (Niles *et al.*, 2014). Given the role ROS play in regulating the actin cytoskeleton (Vilella *et al.*, 2005; confirmed in Figure 1, A and B, by treating wild-type [WT] cells with 1 mM H_2O_2), we tested whether ROS accumulation was involved in actin depolarization after inhibition of Ypk1 signaling. Our approach was to inhibit Ypk1 by treating *ypk1Δ ypk2Δ* cells that expressed an analogue-sensitive allele of Ypk1 (Ypk1-AS) with an ATP-analogue inhibitor for 60 min. As reported previously (Niles *et al.*, 2012), inhibiting Ypk1 kinase activity resulted in a majority of cells displaying either completely depolarized or partially polarized actin (Figure 1, A and B). We observed partial improvement in actin polarization when we treated Ypk1-AS cells with the ROS scavenger *N*-acetyl cysteine (NAC; Figure 1, A and B). This partial improvement in actin polarization is consistent with our previous observation that treatment with NAC results in a partial reduction in ROS (Niles *et al.*, 2014). Deletion of the oxidative stress–induced transcription factor Yap1, required for the removal of ROS (Kuge *et al.*, 1997), exacerbated the actin depolarization phenotype of Ypk1-AS cells (Figure 1, A and B). Taken together, these results suggest that ROS contribute to depolarization of actin in Ypk1-AS cells. A ROS-induced disulfide bond between two conserved cysteine residues in actin (C285 and C374) has been demonstrated to be responsible for depolarization of actin upon oxidative stress (Farah and Amberg, 2007; Lassing

et al., 2007). To test whether direct oxidation of actin is the mechanism that leads to actin depolarization in Ypk1-AS cells, we examined actin polarization of Ypk1-AS cells harboring a mutant allele of *ACT1*, termed *act1^{C374A}*, which is incapable of forming a disulfide bond in the presence of ROS. We observed that expression of *act1^{C374A}*, but not WT *ACT1*, was sufficient to largely reverse the oxidation-induced actin depolarization phenotype of Ypk1-AS cells, indicating that increased ROS leads directly to actin depolarization in Ypk1-AS cells (Figure 1, A and B).

Although these data suggested that ROS accumulation is responsible for actin depolarization in Ypk1-AS cells, we tested the reciprocal hypothesis that actin depolarization was the cause of increased ROS, as mutations in actin that decrease actin dynamics reportedly increase ROS (Gourlay *et al.*, 2004). Accordingly, we examined Ypk1-AS *act1^{C374A}* cells for indirect in vivo levels of ROS with the fluorescent ROS indicator dye 2,7-dichlorofluorescin diacetate (DCF; Lee *et al.*, 2011). Despite rescue of actin polarization by the *act1^{C374A}* mutation, the level of ROS in Ypk1-AS *act1^{C374A}* cells was comparable to that in Ypk1-AS cells (Figure 1C). Thus we conclude that actin depolarization is not responsible for accumulation of ROS in Ypk1-deficient cells.

Because Ypk1 is a downstream kinase of TORC2, which also regulates actin polarization, we examined whether this regulation by TORC2 also involves ROS. Using a temperature-sensitive allele of the essential TORC2 subunit *AVO3*, *avo3-30* (here termed *torc2-ts*), we found that actin depolarization in *torc2-ts* cells was partially rescued by treatment with NAC. We demonstrated further that expression of an allele of Ypk1 (Ypk1^{D242A}; Niles *et al.*, 2012) that bypasses the need for TORC2-dependent phosphorylation restored actin polarization to levels comparable to those of wild-type cells (Figure 1D). Thus, upstream of Ypk1, TORC2 mediates suppression of ROS and maintenance of actin polarization.

Ypk1 regulates actin polarization through Fpk1, sphingolipids, and mitochondria-mediated ROS

To identify components involved in TORC2-Ypk1 regulation of actin polarization, we next examined actin polarization when Ypk1-AS cells were combined with mutations that are known to reduce ROS. We showed previously that inhibition of Ypk1 results in ROS accumulation from multiple sources, with one source being aberrant mitochondrial respiration that is dependent on the protein kinase A (PKA) subunit Tpk3. In addition, a second source of ROS results from defects in vacuolar acidification, which is dependent on the phospholipid flippase kinase Fpk1 (Niles *et al.*, 2014). Remarkably, Ypk1-AS rho^0, Ypk1-AS *fpk1Δ*, and Ypk1-AS *fpk1Δ* rho^0 cells all displayed improved actin polarization that correlated precisely with their reduction in ROS (Niles *et al.*, 2014; Figure 2A). In particular, Ypk1-AS *fpk1Δ* rho^0 cells, which have WT levels of ROS (Niles *et al.*, 2014), displayed completely normal actin polarization (Figure 2A). Furthermore, deletion of the phospholipid flippases *DNF1*, *DNF2*, and *DNF3* or the PKA subunit *TPK3* also restored actin polarization within Ypk1-AS cells in a manner that was consistent with their reduction in ROS (Figure 2A).

As an alternative approach to examine the role of Fpk1 in ROS accumulation and actin polarization, we expressed a hyperactive mutant allele of Fpk1 (Fpk1 3A) that cannot be repressed via phosphorylation by Ypk1 (Roelants *et al.*, 2010). Expression of Fpk1 3A, but not a kinase-dead version of Fpk1 3A (Fpk1 3A KD), both increased ROS (25% of DCF-positive cells) and induced partial depolarization of actin (Figure 2, B and C). Treating Fpk1 3A–expressing cells with NAC both reduced ROS and increased actin polarization (Figure 2, B and C). Moreover, preventing actin oxidation by
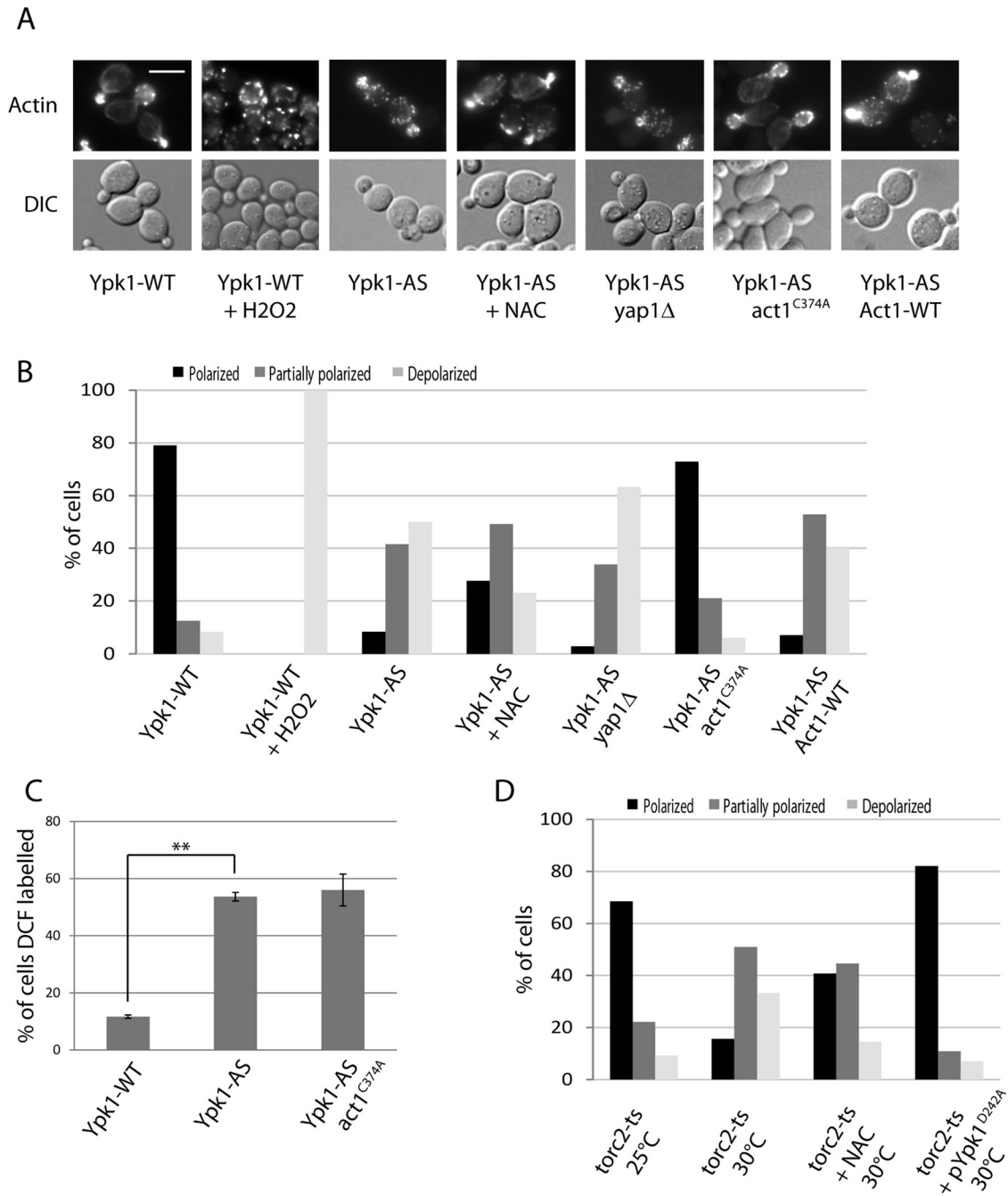
FIGURE 1: Ypk1-dependent ROS perturbs actin cytoskeleton organization. (A) Ypk1-WT (PLY1083), Ypk1-AS (PLY1098), Ypk1-AS *yap1Δ* (PLY1527), Ypk1-AS act1[C374A] (PLY1588), and Ypk1-AS Act1-WT (PLY1626) were grown in SCD-Ura medium, with 20 mM NAC as noted, and then all strains were treated for 1 h with 0.5 μM 2,3-DMB-PPI, and with 1 mM H₂O₂ where noted, and then fixed and labeled for actin with rhodamine-phalloidin. Scale bar, 5 μm. (B) Quantification of actin polarization for the same strains as in A, with at least 100 budded cells counted for each sample. (C) Ypk1-WT (PLY1083), Ypk1-AS (PLY1098), and Ypk1-AS *act1*[C374A] (PLY1588) were grown as in A and incubated for the last 30 min with 10 μM DCF. Quantification represents percentage of 200–300 cells labeled with DCF, including the SD from at least three experiments. *p* values were calculated using Student's *t* test; **$p \leq 0.01$. (D) *torc2-ts* (PLY1134) transformed with empty vector (pPL187) or YPK1[D242A] (pPL240) were grown overnight at 25°C, with 20 mM NAC where noted, and then shifted to 30°C as noted for 1 h. Cells were fixed and labeled for actin with rhodamine-phalloidin as in A and quantified as in B.

expressing the *act1*[C374A] allele was sufficient to restore actin polarization in Fpk1 3A cells, and yet, as expected, did not reduce ROS (Figure 2, B and C). Together these results confirm that Fpk1-mediated ROS leads to actin depolarization by oxidation of Act1.

We demonstrated previously that Ypk1-AS cells have decreased levels of sphingolipids, and that sphingolipids and Fpk1 function antagonistically within the same pathway to regulate ROS accumulation, in part by influencing vacuolar acidification (Niles *et al.*, 2014).
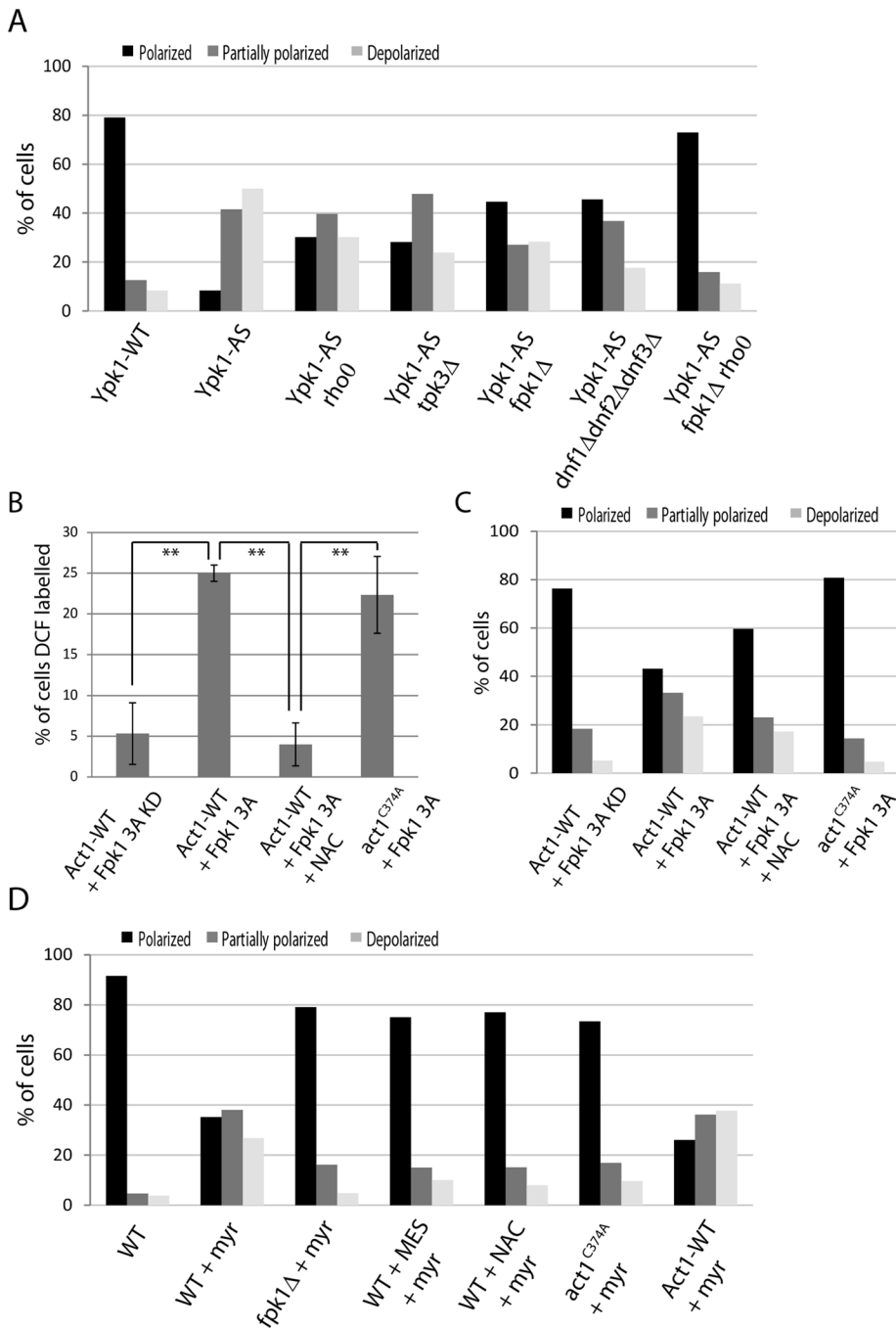
FIGURE 2: Ypk1 regulates actin polarization by suppression of ROS from multiple sources. (A) Ypk1-WT (PLY1083), Ypk1-AS (PLY1098), Ypk1-AS rho[0] (PLY1528), Ypk1-AS *tpk3Δ* (PLY1529), Ypk1-AS *fpk1Δ* (PLY1533), Ypk1-AS *dnf1Δdnf2Δdnf3Δ* (PLY1534), and Ypk1-AS *fpk1Δ* rho[0] (PLY1536) were grown, fixed, and labeled for actin with rhodamine-phalloidin as in Figure 1A and quantified as in Figure 1B. (B) Act1-WT + Fpk1 3A KD (PLY1629), Act1-WT + Fpk1 3A (PLY1630), and act1 C374A + Fpk1 3A (PLY1631) were grown in SCD-Ura-Leu medium, with 20 mM NAC as noted, and then incubated with DCF as in Figure 1C or (C) fixed and labeled for actin and quantified as in A. (D) WT (PLY062), *fpk1Δ* (PLY1440), act1 C374A (PLY1628), and Act1-WT (PLY1627) were grown in SCD, or in SCD + MES as noted, and treated with 1.25 µM myriocin (Myr) for 1 h as noted, fixed, and labeled for actin and quantified as in A.

As sphingolipids are known to regulate actin polarization (Friant *et al.*, 2001), we tested whether this was mediated by suppression of ROS. Indeed, we observed that defects in actin polarization caused by the sphingolipid biosynthesis inhibitor myriocin were restored either by deletion of *FPK1* or by treating cells with the buffer

2-(*N*-morpholino)ethanesulfonic acid (MES; Figure 2D), both of which restore vacuolar acidification and reduce ROS in myriocin-treated cells (Niles *et al.*, 2014). Although cells deleted for *FPK1* have been shown to possess reduced myriocin uptake (Yamane-Sando *et al.*, 2014), we used a concentration of myriocin that is effective even in *fpk1Δ* cells (Roelants *et al.*, 2011). In addition, we were able to restore actin polarization in myriocin-treated cells by directly reducing ROS by treating cells with NAC or, alternatively, by preventing oxidation of actin at C374 (Figure 2D). On the basis of these combined results, we conclude that Ypk1 regulates actin polarization via actin oxidation by ROS produced from multiple sources, including defects in vacuolar acidification mediated by overactive Fpk1 and reduced sphingolipids, as well as by impaired mitochondrial activity.

Pkc1/MAPK activation suppresses ROS and restores actin polarization in Ypk1-deficient cells

Regulation of actin polarization by TORC2-Ypk1 is known to involve components of the Pkc1-MAPK signaling cascade (Helliwell *et al.*, 1998b). In particular, overexpression of Pkc1 or its downstream target Mpk1 rescues actin defects in *ypk1ts* mutant cells (Roelants *et al.*, 2002; Schmelzle *et al.*, 2002). We sought to determine whether ROS-mediated actin depolarization in Ypk1-AS cells was influenced by Pkc1-MAPK signaling. Accordingly, we examined ROS levels in Ypk1-AS cells that expressed an activated allele of Pkc1 (Pkc1[R398P]; Helliwell *et al.*, 1998b). We observed that expression of Pkc1[R398P] resulted in a partial but significant reduction in ROS (31 vs. 54% DCF-positive cells; Figure 3A). ROS was further reduced when Pkc1[R398P] was expressed in Ypk1-AS rho[0] cells (22% DCF-positive cells), suggesting that Pkc1 regulates ROS independently of mitochondrial function (Figure 3A). Consistent with these findings, decreased ROS correlated with improved actin polarization (Figure 3B), indicating that Ypk1 regulates actin polarization in part through Pkc1-dependent ROS.

We next tested whether Fpk1 and Pkc1 interact functionally to regulate ROS and actin polarization in Ypk1-AS cells. Expression of Pkc1[R398P] in Ypk1-AS *fpk1Δ* cells did not further decrease ROS and only subtly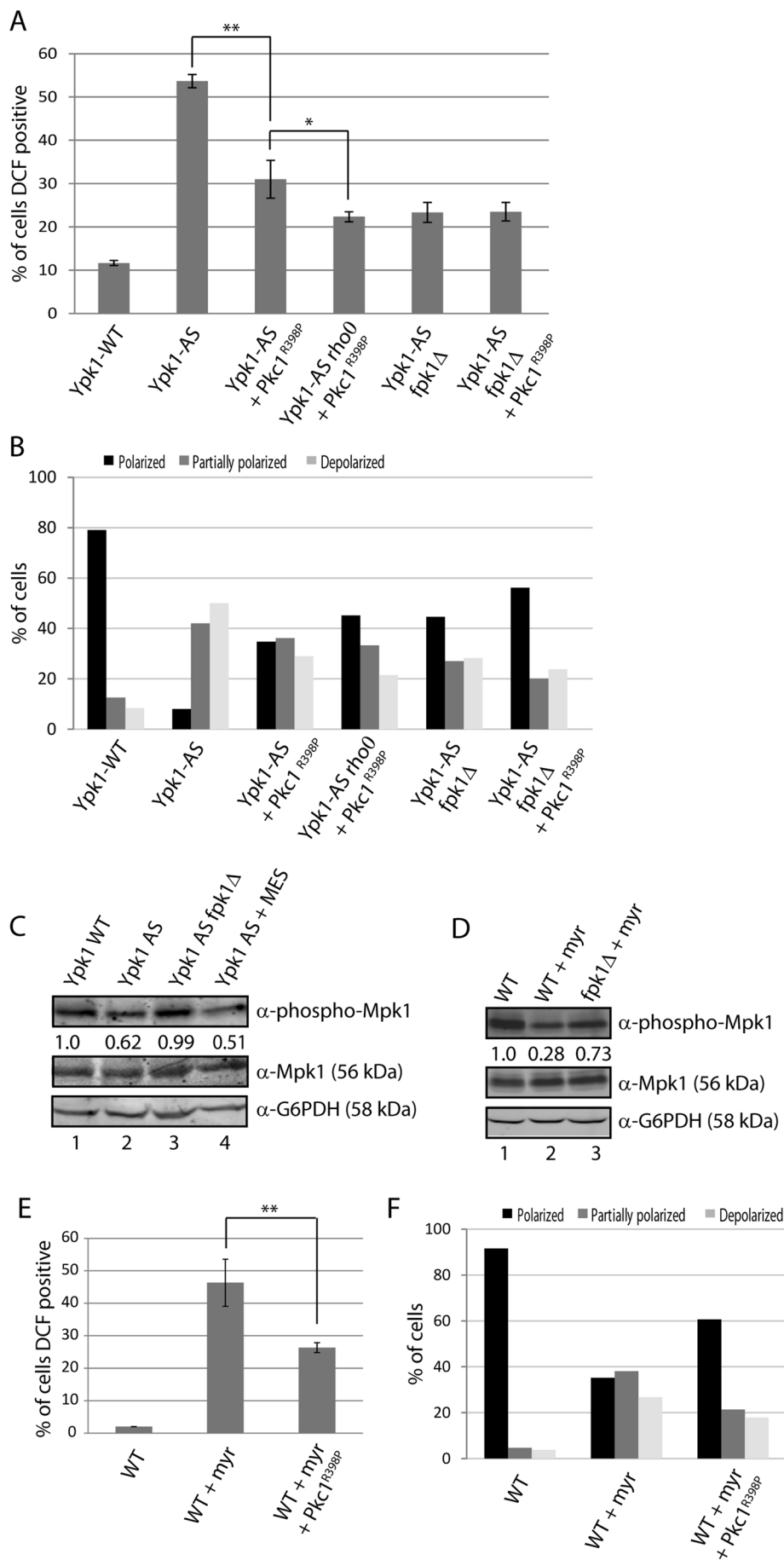 improved actin polarization (Figure 3, A and B). This suggested that Fpk1 and Pkc1 might function within the same pathway to regulate ROS and actin polarization. Accordingly, we tested the possibility that Fpk1 regulates Pkc1, by measuring Pkc1-dependent phosphorylation of Mpk1 (Slt2), a downstream target of Pkc1 signaling (Gustin *et al.*, 1998). Consistent with previous

FIGURE 3: Regulation of ROS by Pkc1 is downstream of Ypk1 and Fpk1. (A) Ypk1-WT (PLY1083), Ypk1-AS (PLY1098), Ypk1-AS + PKC1^{R398P} (1531), Ypk1-AS rho^0 + PKC1^{R398P} (PLY1532), Ypk1-AS $fpk1\Delta$ (PLY1533), and Ypk1-AS $fpk1\Delta$ + PKC1^{R398P} (PLY1538) were grown in either SCD-Ura or SCD-Ura/-Leu medium and treated with 0.5 µM 2,3-DMB-PPI for 1 h. ROS was determined and quantified as in Figure 1C. p values were calculated using Student's t test; *p between 0.05 and 0.01; **$p \leq 0.01$. (B) Quantification of actin polarization after fixing and rhodamine-phalloidin labeling in the same strains as in A, with at least 100 cells counted for each sample. (C) Ypk1-WT (PLY1083), Ypk1-AS (PLY1098), and Ypk1-AS $fpk1\Delta$ (PLY1533) were grown in either SCD-Ura or SCD-Ura + 50 mM MES, pH 6.2, and treated with 0.5 µM 2,3-DMB-PPI for 1 h. Cells were harvested and lysed, and the resulting protein extracts were resolved by SDS–PAGE and immunoblotted with anti–phospho-p44/42 MAPK (for p-Mpk1), anti-Mpk1, and anti-G6PDH antibodies. Quantification below the blot describes the difference relative to Ypk1-WT after normalizing to the anti-p44/p42 MAPK signal. (D) WT (PLY062) and $fpk1\Delta$ (PLY1440) were grown in SCD medium and treated with 1.25 µM myriocin (Myr) for 1 h as noted and then processed as in C. (E) WT (PLY062) and WT + PKC1^{R398P} (PLY1550) were grown in SCD or SCD-Leu medium and treated as in D. ROS was detected and quantified as in Figure 1C. p values were calculated using Student's t test; **$p \leq 0.01$. (F) Quantification of actin polarization after fixing and rhodamine-phalloidin labeling in the same strains as in E, with least 100 cells counted for each sample.

findings that Pkc1 activity is decreased in *torc2/ypk* mutants (Kamada *et al.*, 2005), we observed a reproducible reduction in Mpk1 phosphorylation in Ypk1-AS cells (Figure 3C). Of interest, Mpk1 phosphorylation was restored to WT levels in Ypk1-AS $fpk1\Delta$ cells (Figure 2C), indicating that overactive Fpk1 in Ypk1-AS cells negatively regulates Pkc1/MAPK signaling. Surprisingly, however, restoring vacuolar acidification by treating Ypk1-AS cells with MES did not restore Mpk1 phosphorylation, suggesting that Fpk1 regulates Pkc1/MAPK signaling independently of either intracellular acidification or ROS (Figure 3C). Taking the results together, we conclude that overactive Fpk1 activity in Ypk1-AS cells regulates ROS by two independent mechanisms, through intracellular acidification defects and also by inhibiting Pkc1/MAPK activity.

On the basis of the similar regulation of actin polarization by both Fpk1 and sphingolipids, we examined whether

sphingolipids also played a role in regulating Pkc1 activity. We treated WT cells with myriocin and examined Mpk1 phosphorylation, which we observed was significantly reduced (Figure 3D). Of interest, deletion of *FPK1* largely restored Mpk1 phosphorylation in myriocin-treated cells, suggesting that Fpk1 contributes to sphingolipid-dependent regulation of Pkc1 activity. Because sphingolipids regulate actin polarization through ROS, we tested whether Pkc1 contributed to ROS in sphingolipid-depleted cells. Indeed, we found that overexpression of Pkc1[R398P] in WT cells treated with myriocin partially but significantly reduced ROS (Figure 3E), as well as improved actin polarization (Figure 3F). Taking the results together, we conclude that sphingolipids and Fpk1 cooperate to regulate Pkc1 activity and that this contributes to the suppression of ROS and maintenance of actin polarization.

Pkc1/MAPK activity is regulated by Fpk1- and sphingolipid-dependent localization of Rom2

Pkc1 is activated by Rho1, which, in turn, is regulated by a number of GEFs, including Rom2. Treatment with myriocin is known to disrupt Rom2 localization at the plasma membrane (PM), specifically abolishing its concentration at bud tips (Kobayashi et al., 2005). Because myriocin treatment decreased Pkc1 activity, we tested whether this correlated with mislocalization of Rom2. Indeed, we observed that bud tip recruitment of a green fluorescent protein (GFP)–tagged version of Rom2 was disrupted in Ypk1-AS cells (Figure 4A). On the basis of our finding that sphingolipid levels affect Pkc1 activity, we hypothesized that decreased sphingolipids in Ypk1-AS cells may contribute to the mislocalization of Rom2. We demonstrated previously that addition of the sphingolipid precursor phytosphingosine (PHS) to *torc2-ts* cells that are deleted for *LCB4*, the major LCB kinase, increases synthesis of downstream complex sphingolipids to a level sufficient to restore viability, as well as rescues defects in actin polarization (Aronova et al., 2008). Therefore, we treated Ypk1-AS *lcb4Δ* cells with PHS and examined Rom2-GFP localization; we observed that bud tip recruitment of Rom2 was significantly restored (Figure 4A). Similarly, we observed that bud/neck recruitment of GFP-Rom2 was also improved in Ypk1-AS *fpk1Δ* cells (Figure 4A). Together these data demonstrate that Fpk1 activity and sphingolipids are critical for Ypk1-dependent regulation of Rom2 localization. Of interest, treatment with NAC did not restore Rom2 localization at the PM (Figure 4A), suggesting that sphingolipids and Fpk1 do not regulate Rom2 localization via ROS and/or actin polarization.

We next tested whether Rom2 mislocalization contributed to decreased Pkc1 activity in Ypk1-AS cells. Because deleting *FPK1* from Ypk1-AS resulted in restoration of Rom2 bud/neck recruitment, as well as rescue of Pkc1 activity, we examined whether this rescue of Pkc1 activity required the presence of Rom2. To do this, we deleted *ROM2* from Ypk1-AS *fpk1Δ* cells and examined Pkc1 activity. Indeed, rescue of Pkc1 activity in Ypk1-AS *fpk1Δ* cells required the presence of *ROM2*, as Mpk1 phosphorylation was reduced in Ypk1-AS *fpk1Δ rom2Δ* cells (Figure 4B). Furthermore, the rescue of ROS and actin depolarization that results from deleting *FPK1* from Ypk1-AS cells also required *ROM2* (Figure 4, D and E). Consistent with these findings, we observed that overexpression of *ROM2* in Ypk1-AS cells resulted in increased Mpk1 phosphorylation (Figure 4C), decreased ROS, and improved actin polarization (Figure 4, D and E). Taking these results together, we conclude that restoring Rom2 activity at the PM is crucial for Pkc1 activation, both to rescue ROS and to maintain actin polarization, in Ypk1-deficient cells. In agreement with results of a prior study (Vilella et al., 2005), we observed that loss of Rom2 activity on its own did not result in increased ROS or actin depolarization in *rom2Δ* cells (unpublished data), suggesting

that the Rom2 and Pck1/MAPK branch of the pathway becomes essential within the context of deficient Ypk1 signaling.

Pkc1/MAPK regulates ROS through cyclin C stability

Because the MAPK signaling pathway is one of the best-characterized targets of activated Pkc1, we tested whether Pkc1 regulation of ROS was mediated by MAPK signaling, first by examining the MAPKKK kinase Bck1. We observed that expression of a constitutively active allele of Bck1 (Bck1-20) in Ypk1-AS cells reduced ROS levels similar to that observed by expression of Pkc1[R398P], suggesting that Pkc1 regulates ROS through the MAPK signaling pathway (Figure 5A). Of interest, MAPK signaling has been shown to regulate the oxidative stress response by controlling the stability of cyclin C, a transcriptional repressor that inhibits several stress-responsive genes (Krasley et al., 2006). Accordingly, we deleted *CNC1*, the gene encoding cyclin C, from Ypk1-AS cells and examined ROS levels. Consistent with a role for MAPK in mediating ROS through cyclin C, Ypk1-AS *cnc1Δ* cells exhibited significant reduction in ROS compared with Ypk1-AS cells (22 vs. 55% DCF-positive cells; Figure 5A). Cyclin C regulates transcription by activation of the cyclin-dependent kinase Cdk8 but has also been shown to regulate ROS independently of Cdk8 (Krasley et al., 2006). No change in ROS was observed in Ypk1-AS cells after deletion of *CDK8*, indicating that cyclin C is likely to regulate ROS by a mechanism that is independent of Cdk8-mediated transcription (Figure 5A). Consistent with these findings, we observed that actin polarization was improved in Ypk1-AS cells by expression of Bck1-20 or deletion of *CNC1* but not by deletion of *CDK8* (Figure 5B).

On oxidative stress, cyclin C is degraded to promote activation of oxidative stress responses (Krasley et al., 2006). On the basis of our foregoing results, we tested whether Ypk1-AS cells exhibited a defect in the regulation of cyclin C stability. Specifically, we examined cyclin C protein levels after treatment with H_2O_2, using a myc-epitope tagged version of cyclin C (Cooper et al., 1997). In agreement with previous findings (Krasley et al., 2006), cyclin C levels were reduced in WT cells by treatment with H_2O_2 but not in *mpk1Δ* cells (Figure 5C). This finding confirmed a requirement for Pkc1-MAPK signaling in ROS-mediated cyclin C degradation. Significantly, Ypk1-AS cells exhibited increased cyclin C levels compared with Ypk1-WT cells, and, in addition, treatment with H_2O_2 failed to decrease cyclin C levels, consistent with Ypk1-AS cells possessing reduced Pkc1 activity. Furthermore, we observed that restoring Pkc1 activity in Ypk1-AS cells, either by deleting *FPK1* or by treating Ypk1-AS *lcb4Δ* cells with PHS, resulted in cyclin C degradation after treatment with H_2O_2 (Figure 5C). Together these results suggest that Pkc1-mediated degradation of cyclin C is important for the regulation of ROS and actin polarization in Ypk1-deficient cells.

DISCUSSION

Our data presented here identify ROS as a crucial mediator of TORC2/Ypk1 regulation of actin polarization. Our findings support a model in which TORC2/Ypk1 regulation of Fpk1, sphingolipids, and mitochondrial respiration combines to prevent ROS-induced oxidation of critical cysteine residues on actin (Figure 6). We also find that Fpk1 and sphingolipids regulate Pkc1 activity by influencing the localization of Rom2 at the PM, and Pkc1 in turn regulates ROS through MAPK-dependent destruction of cyclin C protein. Thus, whereas Pkc1-MAPK signaling is known to function downstream of TORC2 to regulate actin polarization, our findings demonstrate that ROS is a critical determinant within this pathway.
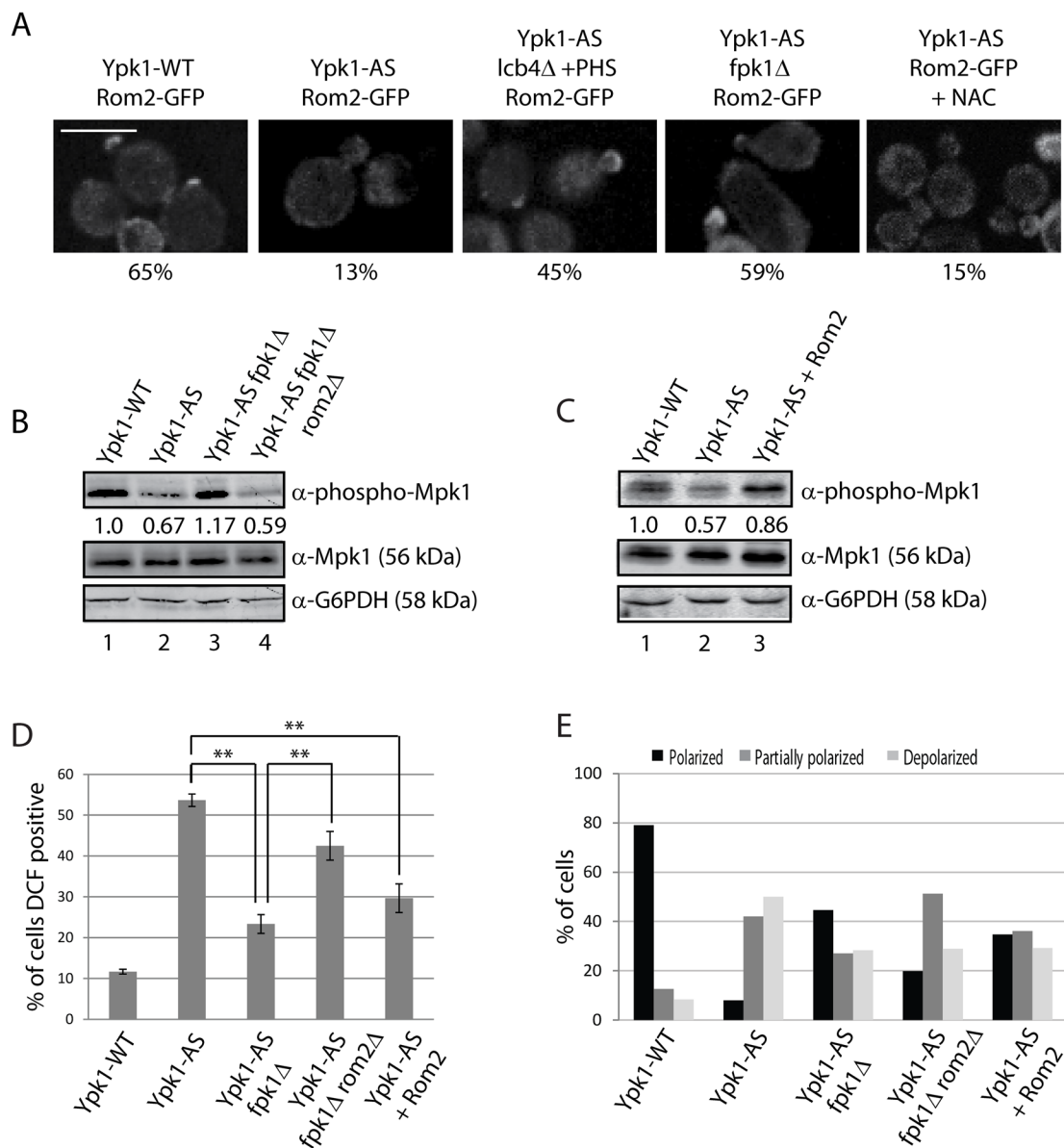
FIGURE 4: Regulation of Pkc1/MAPK activity requires Fpk1- and sphingolipid-dependent PM localization of Rom2. (A) Ypk1-WT *rom2Δ* + ROM2-GFP (PLY1563), Ypk1-AS *rom2Δ* + ROM2-GFP (PLY1564), Ypk1-AS *lcb4Δ rom2Δ* + ROM2-GFP (PLY1566), and Ypk1-AS *fpk1Δ rom2Δ* + ROM2-GFP (PLY1565) cells were grown in SCD-Ura/-Leu medium, with 4 μM PHS or 20 mM NAC where noted, and treated with 0.5 μM 2,3-DMB-PPI for 1 h. Single focal plane images were collected by confocal microscopy. Quantification represents percentage of small-budded cells labeled with GFP, with 30–50 cells counted for each sample. Scale bar, 5 μm. (B) Ypk1-WT (PLY1083), Ypk1-AS (PLY1098), Ypk1-AS *fpk1Δ* (PLY1533), and Ypk1-AS *fpk1Δ rom2Δ* (PLY1561) were grown in SCD-Ura medium and treated with 0.5 μM 2,3-DMB-PPI for 1 h. Cells were harvested and lysed, and the resulting protein extracts were resolved by SDS/PAGE and immunoblotted with anti-phospho-p44/42 MAPK (for p-Mpk1), anti-Mpk1, and anti-G6PDH antibodies. Quantification below the blot describes the difference relative to Ypk1-WT after normalizing to the anti-p44/p42 MAPK signal. (C) Ypk1-WT (PLY1083), Ypk1-AS (PLY1098), and Ypk1-AS + Rom2-HA (PLY1568) were grown in SCD-Ura medium, treated with 0.5 μM 2,3-DMB-PPI for 1 h, and then processed as in B. (D) Ypk1-WT (PLY1083), Ypk1-AS (PLY1098), Ypk1-AS *fpk1Δ* (PLY1533), Ypk1-AS *fpk1Δ rom2Δ* (PLY1561), and Ypk1-AS + ROM2-HA (PLY1568) were grown in SCD-Ura medium and treated with 0.5 μM 2,3-DMB-PPI for 1 h. ROS was determined and quantified as in Figure 1C. *p* values were calculated using Student's *t* test; **$p \leq 0.01$. (E) Quantification of actin polarization after fixing and rhodamine-phalloidin labeling in the same strains as in D, with at least 100 cells counted for each sample.

Pkc1/MAPK signaling is induced after oxidative stress and is an important part of the cellular response to ROS (Pujol-Carrion *et al.*, 2013; Vilella *et al.*, 2005). By contrast, we observed that increased ROS correlates with decreased Pkc1 activity in Ypk1-deficient cells.

Because Rom2 is required for activation of Pkc1, our observation that Rom2 is mislocalized in Ypk1-AS cells can account for this defect in Pkc1 activation. In addition, our findings that restoring sphingolipid levels or deletion of *FPK1* is sufficient to restore Rom2 localization
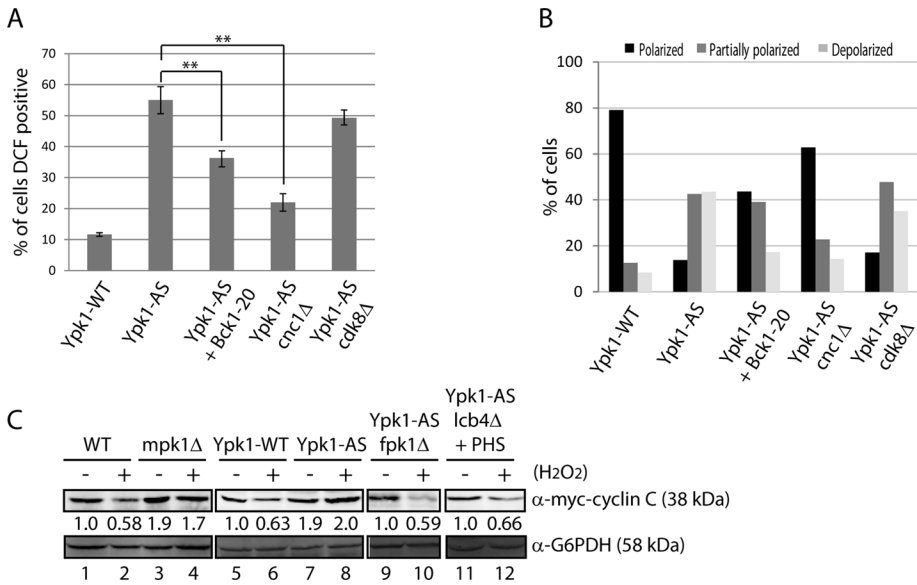
FIGURE 5: Pkc1/MAPK regulates ROS through cyclin C protein stability. (A) Ypk1-WT (PLY1083), Ypk1-AS (PLY1098), Ypk1-AS + Bck1-20 (PLY1585), Ypk1-AS *cnc1Δ* (PLY1586), and Ypk1-AS *cdk8Δ* (PLY1587) were grown in either SCD-Ura or SCD-Ura/-Leu and treated with 0.5 μM 2,3-DMB-PPI for 1 h. ROS was determined and quantified as in Figure 1C. *p* values were calculated using Student's *t* test; **$p \leq 0.01$. (B) Quantification of actin polarization after fixing and rhodamine-phalloidin labeling in the same strains as in A, with at least 100 cells counted for each sample. (C) WT (PLY062), mpk1Δ (PLY517), Ypk1-WT (PLY1083), Ypk1-AS (PLY1098), Ypk1-AS *fpk1Δ* (PLY1533), and Ypk1-AS *lcb4Δ* (PLY1556) cells all expressing myc-tagged cyclin C (pRL101) were grown in 0.5-l cultures of SCD-Leu medium, treated with 0.5 μM 2,3-DMB-PPI for 1 h, and treated with 0.2M H_2O_2 where noted. Total protein lysates and myc immunoprecipitates were resolved by SDS–PAGE and immunoblotted with anti-myc and anti-G6PDH antibodies. Quantification below the blot describes the difference relative to its control after normalizing to the anti-G6PDH signal.

phatidylinositol phosphate kinase Mss4 (Kobayashi *et al.*, 2005). Thus mislocalization of Rom2 in Ypk1-AS cells is consistent with decreased sphingolipids and presumably decreased PIP2 levels within these cells. Precisely how Fpk1 activity influences Rom2 localization, however, remains to be determined. Based on its known function as a regulator of phospholipid flippase activity, it is possible that deletion of *FPK1* results in PM phospholipid remodeling to enable sufficient availability or accessibility of PIP2 to Rom2. In this context, Fpk1 has been shown to regulate the localization and activity of another bud-tip-localized protein, Cdc42, by modulating the phospholipids phosphatidylethanolamine and phosphatidylserine (Saito *et al.*, 2007). Because Rom2 regulates Pck1 via activation of Rho1, which also localizes to bud tips, another possibility is that Fpk1-dependent modulation of phospholipid distribution regulates Rho1 directly. Of interest, a recent study implicated Pkc1 in the regulation of membrane fluidity by determining phospholipid acyl group composition (Lockshon *et al.*, 2012). Thus one intriguing possibility is that phospholipid composition and distribution within the lipid bilayer are interconnected by functional interactions between Pkc1 and Fpk1 and that this is critical for maintenance of membrane homeostasis.

Regulation of ROS by Pkc1 provides an explanation for the observation that overexpression of Pkc1 restores actin polarization in *torc2/ypk1* mutants (Helliwell *et al.*, 1998a; Roelants *et al.*, 2002). Previous studies showed that MAPK signaling is required to regulate the cellular response to oxidative stress by modulating cyclin C protein levels. We extended these findings by showing that misregulation of cyclin C degradation leads to an increase in ROS in Ypk1-deficient cells. MAPK phosphorylation is necessary for cyclin C nuclear-to-cytoplasmic translocation, where cyclin C destruction occurs (Cooper *et al.*, 2012; Jin *et al.*, 2014). Cyclin C is known to repress the activity of stress response genes, including catalase and several protein chaperones (Cooper *et al.*, 1997; Holstege *et al.*, 1998), whose absence could lead to an increase in ROS. However, we found that deleting the gene for Cdk8, the cyclin-dependent kinase that partners with cyclin C, does not affect ROS. Thus either cyclin C represses transcription of target genes independently of Cdk8 or cyclin C regulates ROS by a mechanism that is distinct from transcription.

Cytoskeletal organization in mammalian cells is regulated by mTORC2 and involves Rho GTPases and PKC (Jacinto *et al.*, 2004; Li and Gao, 2014), which leads us to speculate that TORC2/Ypk1 regulation of actin organization by ROS is likely to be conserved. Consistent with a role for mTORC2 in the regulation of the actin cytoskeleton, mTORC2 is required for neutrophil migration toward chemoattractants (He *et al.*, 2013). Of importance, mTORC2 regulation of actin has also been associated with increased cancer cell migration and invasion (Gupta *et al.*, 2013). Because ROS is also associated with regulation of cell motility, our findings provide novel insight that may be useful in understanding the mechanisms involved in mTORC2-dependent cell

indicate that membrane lipid composition is an important factor for Rom2 activity. Rom2 localization is dependent on phosphatidylinositol 4,5-bisphosphate (PIP2) at the PM, and sphingolipids have been shown to regulate PIP2 levels by regulating the activity of the phos-
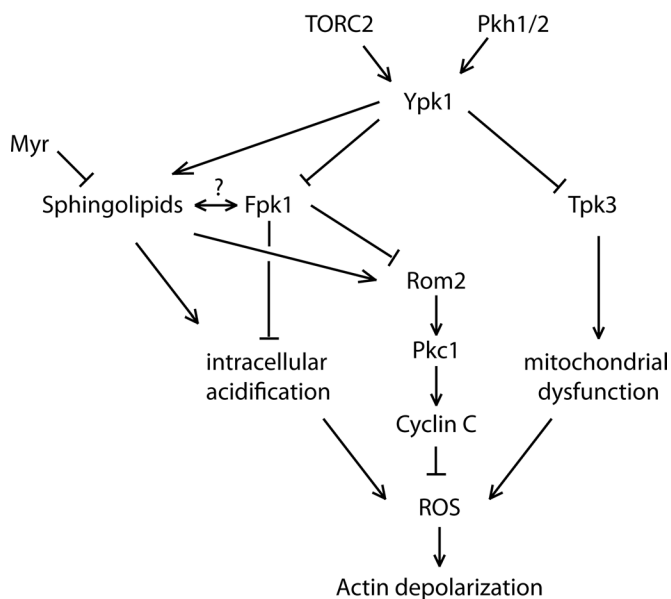

FIGURE 6: Model for TORC2/Ypk1-dependent regulation of ROS and actin polarization. See the text for details.

Strain	Genotype	Source	Strain	Genotype	Source
PLY062	W303α	Nasmyth et al. (1990)	PLY1561	W303α, except ypk1::TRP1 ypk2::HIS3 rom2:: KanMX + [pPL251]	This study
PLY517	W303α, except mpk1::KanMX	Aronova et al. (2007)	PLY1563	W303α, except ypk1::TRP1 ypk2::HIS3 rom2::KanMX + [pPL250] + [pYO2518]	This study
PLY1083	W303α, except ypk1::TRP1 ypk2::HIS3 + [pPL216]	Niles et al. (2012)	PLY1564	W303α, except ypk1::TRP1 ypk2::HIS3 rom2:: KanMX + [pPL251] + [pYO2518]	This study
PLY1098	W303α, except ypk1::TRP1 ypk2::HIS3 + [pPL220]	Niles et al. (2014)	PLY1565	W303α, except ypk1::TRP1 ypk2::HIS3 fpk1::NAT rom2:: KanMX + [pPL251] + [pYO2518]	This study
PLY1134	W303α, except avo3-30-MYC:TRP1	Niles et al. (2012)	PLY1566	W303α, except ypk1::TRP1 ypk2::HIS3 lcb4::markerless rom2::KanMX + [pPL251] + [pYO2518]	This study
PLY1440	W303a, except fpk1::KanMX	Niles et al. (2012)			
PLY1527	W303α, except ypk1::TRP1 ypk2::HIS3 yap1::KanMX + [pPL220]	Niles et al. (2014)	PLY1568	W303α, except ypk1::TRP1 ypk2::HIS3 + [pPL251] + [pAS32]	This study
PLY1528	W303α, except ypk1::TRP1 ypk2::HIS3 rho⁰ + [pPL220]	Niles et al. (2014)	PLY1585	W303α, except ypk1::TRP1 ypk2::HIS3 + [pPL220] + [pPL586]	This study
PLY1529	W303α, except ypk1::TRP1 ypk2::HIS3 tpk3::KanMX + [pPL220]	Niles et al. (2014)	PLY1586	W303α, except ypk1::TRP1 ypk2::HIS3 cnc1::KanMX + [pPL220]	This study
PLY1531	W303α, except ypk1::TRP1 ypk2::HIS3 + [pPL220] + [pPL474]	This study	PLY1587	W303α, except ypk1::TRP1 ypk2::HIS3 cdk8::KanMX + [pPL220]	This study
PLY1532	W303α, except ypk1::TRP1 ypk2::HIS3 rho⁰ + [pPL220] + [pPL474]	This study	PLY1588	W303α, except ypk1::TRP1 ypk2::HIS3 act1::KanMX + [pPL251] + [pPL593]	This study
PLY1533	W303α, except ypk1::TRP1 ypk2::HIS3 fpk1::KanMX + [pPL220]	Niles et al. (2014)	PLY1626	W303α, except ypk1::TRP1 ypk2::HIS3 act1::KanMX + [pPL251] + [pPL592]	This study
PLY1534	W303α, except ypk1::TRP1 ypk2::HIS3 dnf3::markerless dnf2::NAT dnf1::KanMX + [pPL220]	Niles et al. (2014)	PLY1627	W303α, except act1::KanMX + [pPL592]	This study
PLY1536	W303α, except ypk1::TRP1 ypk2::HIS3 fpk1::KanMX rho⁰+ [pPL220]	Niles et al. (2014)	PLY1628	W303α, except act1::KanMX + [pPL593]	This study
PLY1538	W303α, except ypk1::TRP1 ypk2::HIS3 fpk1::NAT + [pPL220] + [pPL474]	This study	PLY1629	W303α, except act1::KanMX + [pPL592] + [pPL603]	This study
			PLY1630	W303α, except act1::KanMX + [pPL592] + [pPL602]	This study
PLY1550	W303α + [pPL474]	This study	PLY1631	W303α, except act1::KanMX + [pPL593] + [pPL602]	This study
PLY1556	W303α, except ypk1::TRP1 ypk2::HIS3 lcb4:: KanMX + [pPL220]	Niles et al. (2014)			

TABLE 1: *Saccharomyces cerevisiae* strains used in this study.

migration and provide new targets for preventing or limiting invasion of cancer cells.

MATERIALS AND METHODS
Strains, media, and plasmids
Yeast strains and plasmids used in this study are listed in Tables 1 and 2, respectively. Culture medium used was synthetic complete dextrose (SCD; 0.8% yeast nitrogen base without amino acids, pH 5.5, 2% dextrose) supplemented with amino acids as described previously (Sherman, 1991). All yeast transformations were conducted using a lithium acetate procedure (Geitz and Woods, 1998). Strains were made respiratory deficient (rho⁰) by treating with 25 μg/ml ethidium bromide for 16 h, as described in Fox et al. (1991). Construction of deletion strains by replacement of complete open

reading frames (ORFs) with a selectable marker was performed as described previously (Dilova et al., 2004) or by replacement of the ORF with the reusable Kanʳ marker as described in Guldener et al. (1996). Construction of expression plasmids was performed by PCR amplification, with mutations introduced by PCR SOEing. pPL602 and pPL603 were made by PCR amplifying the mutated Fpk1 3A and Fpk1 3A KD coding regions from yeast strains YFR235 and YFR237 (Roelants et al., 2010), respectively, and ligating these into pRS315Met25.

Actin labeling and fluorescence microscopy
Actin labeling and detection in yeast cells was performed as described previously (Aronova et al., 2008). For quantification of status of actin polarization, at least 100 small- and medium-budded

Plasmid	Parent vector	Insert/ORF	Source
pRS315			Sikorski and Heiter (1989)
pRS315Met25			Niles et al. (2012)
pRS316			Sikorski and Heiter (1989)
pRS425			Sikorski and Heiter (1989)
pYO2518		ROM2-GFP	Abe et al. (2003)
pAS32		ROM2-HA	Schmidt et al. (1997)
pLR101		CNC1-myc	Cooper et al. (1997)
pPL216	pRS316	YPK1	Niles et al. (2012)
pPL220	pRS316	YPK1^{L424G}	Niles et al. (2014)
pPL250	pRS315	YPK1	Niles et al. (2012)
pPL251	pRS315	YPK1^{L424G}	Niles et al. (2012)
pPL474	pRS425	PKC1^{R398P}	This study
pPL586	pRS425	BCK1^{A3520P}	This study
pPL592	pRS316	ACT1	This study
pPL593	pRS316	ACT1^{C374A}	This study
pPL602	pRS315Met25	FPK1$^{S37A\ T244A\ S481A}$	This study
pPL603	pRS315Met25	FPK1$^{S37A\ T244A\ S481A\ D621A}$	This study

TABLE 2: Plasmids used in this study.

cells were counted for each condition. Cells were considered as polarized if actin patches were concentrated in the bud and five or fewer patches were found in the mother cell. Cells were considered as partially polarized if actin patches were concentrated in the bud and there were more than five patches in the mother cell. Cells were considered as depolarized if patches were evenly distributed in both the bud and the mother cell. DA and 5(6)CFDA imaging was performed using a Nikon E600 fluorescence microscope as described (Niles et al., 2012). Fluorescent protein imaging was performed using the spinning-disk module of a Marianas SDC Real Time 3D Confocal-TIRF microscope (Intelligent Imaging Innovations, 3i) as described (Niles et al., 2012). Image capture and processing was done using SlideBook5 software (3i) and Photoshop (Adobe).

Cyclin C immunoprecipitation
Yeast strains expressing myc-tagged cyclin C were grown in 0.5-l cultures at 30°C to 0.5 OD$_{600}$/ml in SCD without leucine and treated with 0.2 mM H$_2$O$_2$ as noted. Cells were pelleted and washed in H$_2$O and then in yeast extract buffer (YEB; 50 mM 4-(2-hydroxyethyl)-1-piperazineethanesulfonic acid–KOH, pH 7.1, 100 mM β-glycerolphosphate, 50 mM NaF, 5 mM ethylene glycol tetraacetic acid, 5 mM EDTA, 10% glycerol, 0.25% Tween 20, and 150 mM KCl).

Pellets were resuspended 1:1 (wt/vol) in YEB containing protease inhibitors (cocktail tablet; Roche), 2 mM dithiothreitol, and 2 mM phenylmethylsulfonyl fluoride, and cell lysates were frozen into pellets by dripping into liquid nitrogen. These pellets were then beat in a freezer mill (6970EFM; SPEX Sample Prep) three times for 1 min. On thawing, the lysate was spun two times for 20 min at 14,000 × g at 4°C. Two milligrams of total protein was incubated with α-myc antibody (9E10; Covance) and rotated for 2 h at 4°C before incubation with YEB-washed Protein G Sepharose beads. Bound beads were resuspended in SDS-sample buffer and boiled to remove bound protein. "Input" samples of 50 µg of total yeast protein and "precipitation" samples were separated by 10% SDS–PAGE, followed by Western blotting using the same anti-myc antibody (1:1000) and anti–glucose-6-phosphate dehydrogenase (G6PDH; 1:100,000; Sigma-Aldrich).

Western blotting
Protein extracts from at least three separate experiments were prepared using the NaOH cell lysis method (Dilova et al., 2004), loaded onto SDS–PAGE gels, and transferred to nitrocellulose membrane. Membranes were probed with anti–phospho-p44/42 MAPK (1:1000; Cell Signaling Technology), anti-Mpk1 (1:1000; Santa Cruz Biotechnology), and anti-G6PDH (1:100,000; Sigma-Aldrich) primary antibodies and visualized using the appropriate secondary antibodies conjugated to IRDye (1:5000; LI-COR Biosciences) on the Odyssey Infrared Imaging System (LI-COR Biosciences). Images were quantified using ImageQuant software (GE Healthcare).

Statistical analysis
Averages are presented with means ± SD. The p values were calculated using Student's t test; *p between 0.05 and 0.01, **p ≤ 0.01.

REFERENCES
Abe M, Qadota H, Hirata A, Ohya Y (2003). Lack of GTP-bound Rho1p in secretory vesicles of Saccharomyces cerevisiae. J Cell Biol 162, 85–97.

Aronova S, Wedaman K, Anderson S, Yates J 3rd, Powers T (2007). Probing the membrane environment of the TOR kinases reveals functional interactions between TORC1, actin, and membrane trafficking in Saccharomyces cerevisiae. Mol Biol Cell 18, 2779–2794.

Aronova S, Wedaman K, Aronov PA, Fontes K, Ramos K, Hammock BD, Powers T (2008). Regulation of ceramide biosynthesis by TOR complex 2. Cell Metab 7, 148–158.

Bickle M, Delley PA, Schmidt A, Hall MN (1998). Cell wall integrity modulates RHO1 activity via the exchange factor ROM2. EMBO J 17, 2235–2245.

Cooper KF, Mallory MJ, Smith JB, Strich R (1997). Stress and developmental regulation of the yeast C-type cyclin Ume3p (Srb11p/Ssn8p). EMBO J 16, 4665–4675.

Cooper KF, Scarnati MS, Krasley E, Mallory MJ, Jin C, Law MJ, Strich R (2012). Oxidative-stress-induced nuclear to cytoplasmic relocalization is required for Not4-dependent cyclin C destruction. J Cell Sci 125, 1015–1026.

deHart AKA, Schnell JD, Allen DA, Tsai J-Y, Hicke L (2003). Receptor internalization in yeast requires the Tor2-Rho1 signaling pathway. Mol Biol Cell 14, 4676–4684.

Dilova I, Aronova S, Chen JC, Powers T (2004). Tor signaling and nutrient-based signals converge on Mks1p phosphorylation to regulate expression of Rtg1.Rtg3p-dependent target genes. J Biol Chem 279, 46527–46535.

Farah ME, Amberg DC (2007). Conserved actin cysteine residues are oxidative stress sensors that can regulate cell death in yeast. Mol Biol Cell 18, 1359–1365.

Fiaschi T, Cozzi G, Raugei G, Formigli L, Ramponi G, Chiarugi P (2006). Redox regulation of beta-actin during integrin-mediated cell adhesion. J Biol Chem 281, 22983–22991.

Fox TD, Folley LS, Mulero JJ, McMullin TW, Thorsness PE, Hedin LO, Costanzo MC (1991). Analysis and manipulation of yeast mitochondrial genes. Methods Enzymol 194, 149–165.

Friant S, Lombardi R, Schmelzle T, Hall MN, Riezman H (2001). Sphingoid base signaling via Pkh kinases is required for endocytosis in yeast. EMBO J 20, 6783–6792.

Geitz RD, Woods RA (1998). Transformation of yeast by the lithium acetate/ single-stranded carrier DNA/ polyethylene glycol method. In: Methods in Microbiology, ed. AJP Brown and MF Tuite, New York: Academic Press, 53–66.

Gourlay CW, Carpp LN, Timpson P, Winder SJ, Ayscough KR (2004). A role for the actin cytoskeleton in cell death and aging in yeast. J Cell Biol 164, 803–809.

Guldener U, Heck S, Fielder T, Beinhauer J, Hegemann JH (1996). A new efficient gene disruption cassette for repeated use in budding yeast. Nucleic Acids Res 24, 2519–2524.

Gupta S, Hau AM, Beach JR, Harwalker J, Mantuano E, Gonias SL, Egelhoff TT, Hansel DE (2013). Mammalian target of rapamycin complex 2 (mTORC2) is a critical determinant of bladder cancer invasion. PLoS One 8, e81081.

Gustin MC, Albertyn J, Alexander M, Davenport K (1998). MAP kinase pathways in the yeast Saccharomyces cerevisiae. Microbiol Mol Biol Rev 62, 1264–1300.

He Y, Li D, Cook SL, Yoon MS, Kapoor A, Rao CV, Kenis PJ, Chen J, Wang F (2013). Mammalian target of rapamycin and Rictor control neutrophil chemotaxis by regulating Rac/Cdc42 activity and the actin cytoskeleton. Mol Biol Cell 24, 3369–3380.

Helliwell SB, Howald I, Barbet N, Hall MN (1998a). TOR2 is part of two related signaling pathways coordinating cell growth in Saccharomyces cerevisiae. Genetics 148, 99–112.

Helliwell SB, Schmidt A, Ohya Y, Hall MN (1998b). The Rho1 effector Pkc1, but not Bni1, mediates signalling from Tor2 to the actin cytoskeleton. Curr Biol 8, 1211–1214.

Holstege FC, Jennings EG, Wyrick JJ, Lee TI, Hengartner CJ, Green MR, Golub TR, Lander ES, Young RA (1998). Dissecting the regulatory circuitry of a eukaryotic genome. Cell 95, 717–728.

Ikenoue T, Inoki K, Yang Q, Zhou X, Guan KL (2008). Essential function of TORC2 in PKC and Akt turn motif phosphorylation, maturation and signalling. EMBO J 27, 1919–1931.

Jacinto E, Loewith R, Schmidt A, Lin S, Ruegg MA, Hall A, Hall MN (2004). Mammalian TOR complex 2 controls the actin cytoskeleton and is rapamycin insensitive. Nat Cell Biol 6, 1122–1128.

Jin C, Strich R, Cooper KF (2014). Slt2p phosphorylation induces cyclin C nuclear to cytoplasmic translocation in response to oxidative stress. Mol Biol Cell 25, 1396–1407.

Kamada Y, Fujioka Y, Suzuki NN, Inagaki F, Wullschleger S, Loewith R, Hall MN, Ohsumi Y (2005). Tor2 directly phosphorylates the AGC kinase Ypk2 to regulate actin polarization. Mol Cell Biol 25, 7239–7248.

Kobayashi T, Takematsu H, Yamaji T, Hiramoto S, Kozutsumi Y (2005). Disturbance of sphingolipid biosynthesis abrogates the signaling of Mss4, phosphatidylinositol-4-phosphate 5-kinase, in yeast. J Biol Chem 280, 18087–18094.

Krasley E, Cooper KF, Mallory MJ, Dunbrack R, Strich R (2006). Regulation of the oxidative stress response through Slt2p-dependent destruction of cyclin C in Saccharomyces cerevisiae. Genetics 172, 1477–1486.

Kuge S, Jones N, Nomoto A (1997). Regulation of yAP-1 nuclear localization in response to oxidative stress. EMBO J 16, 1710–1720.

Lassing I, Schmitzberger F, Bjornstedt M, Holmgren A, Nordlund P, Schutt CE, Lindberg U (2007). Molecular and structural basis for redox regulation of beta-actin. J Mol Biol 370, 331–348.

Lee ME, Singh K, Snider J, Shenoy A, Paumi CM, Stagljar I, Park HO (2011). The Rho1 GTPase acts together with a vacuolar glutathione S-conjugate transporter to protect yeast cells from oxidative stress. Genetics 188, 859–870.

Li X, Gao T (2014). mTORC2 phosphorylates protein kinase Czeta to regulate its stability and activity. EMBO Rep 15, 191–198.

Lockshon D, Olsen CP, Brett CL, Chertov A, Merz AJ, Lorenz DA, Van Gilst MR, Kennedy BK (2012). Rho signaling participates in membrane fluidity homeostasis. PLoS One 7, e45049.

Mammoto A, Ingber DE (2009). Cytoskeletal control of growth and cell fate switching. Curr Opin Cell Biol 21, 864–870.

Mooren OL, Galletta BJ, Cooper JA (2012). Roles for actin assembly in endocytosis. Annu Rev Biochem 81, 661–686.

Moseley JB, Goode BL (2006). The yeast actin cytoskeleton: from cellular function to biochemical mechanism. Microbiol Mol Biol Rev 70, 605–645.

Nasmyth K, Adolf G, Lydall D, Seddon A (1990). The identification of a second cell cycle control on the HO promoter in yeast: cell cycle regulation of SW15 nuclear entry. Cell 62, 631–647.

Niles BJ, Joslin AC, Fresques T, Powers T (2014). TOR complex 2-Ypk1 signaling maintains sphingolipid homeostasis by sensing and regulating ROS accumulation. Cell Rep 6, 541–552.

Niles BJ, Mogri H, Hill A, Vlahakis A, Powers T (2012). Plasma membrane recruitment and activation of the AGC kinase Ypk1 is mediated by target of rapamycin complex 2 (TORC2) and its effector proteins Slm1 and Slm2. Proc Natl Acad Sci USA 109, 1536–1541.

Nonaka H, Tanaka K, Hirano H, Fujiwara T, Kohno H, Umikawa M, Mino A, Takai Y (1995). A downstream target of RHO1 small GTP-binding protein is PKC1, a homolog of protein kinase C, which leads to activation of the MAP kinase cascade in Saccharomyces cerevisiae. EMBO J 14, 5931–5938.

Park SJ, Kim YT, Jeon YJ (2012). Antioxidant dieckol downregulates the Rac1/ROS signaling pathway and inhibits Wiskott-Aldrich syndrome protein (WASP)-family verprolin-homologous protein 2 (WAVE2)-mediated invasive migration of B16 mouse melanoma cells. Mol Cells 33, 363–369.

Pujol-Carrion N, Petkova MI, Serrano L, de la Torre-Ruiz MA (2013). The MAP kinase Slt2 is involved in vacuolar function and actin remodeling in Saccharomyces cerevisiae mutants affected by endogenous oxidative stress. Appl Environ Microbiol 79, 6459–6471.

Roelants FM, Baltz AG, Trott AE, Fereres S, Thorner J (2010). A protein kinase network regulates the function of aminophospholipid flippases. Proc Natl Acad Sci USA 107, 34–39.

Roelants FM, Breslow DK, Muir A, Weissman JS, Thorner J (2011). Protein kinase Ypk1 phosphorylates regulatory proteins Orm1 and Orm2 to control sphingolipid homeostasis in Saccharomyces cerevisiae. Proc Natl Acad Sci USA 108, 19222–19227.

Roelants FM, Torrance PD, Bezman N, Thorner J (2002). Pkh1 and pkh2 differentially phosphorylate and activate ypk1 and ykr2 and define protein kinase modules required for maintenance of cell wall integrity. Mol Biol Cell 13, 3005–3028.

Saito K, Fujimura-Kamada K, Hanamatsu H, Kato U, Umeda M, Kozminski KG, Tanaka K (2007). Transbilayer phospholipid flipping regulates Cdc42p signaling during polarized cell growth via Rga GTPase-activating proteins. Dev Cell 13, 743–751.

Schmelzle T, Helliwell SB, Hall MN (2002). Yeast protein kinases and the RHO1 exchange factor TUS1 are novel components of the cell integrity pathway in yeast. Mol Cell Biol 22, 1329–1339.

Schmidt A, Bickle M, Beck T, Hall MN (1997). The yeast phosphatidylinositol kinase homolog TOR2 activates RHO1 and RHO2 via the exchange factor ROM2. Cell 88, 531–542.

Shartava A, Monteiro CA, Bencsath FA, Schneider K, Chait BT, Gussio R, Casoria-Scott LA, Shah AK, Heuerman CA, Goodman SR (1995). A post-translational modification of beta-actin contributes to the slow dissociation of the spectrin-protein 4.1-actin complex of irreversibly sickled cells. J Cell Biol 128, 805–818.

Sherman F (1991). Getting started with yeast. Methods Enzymol 194, 3–21.

Shimada K, Filipuzzi I, Stahl M, Helliwell SB, Studer C, Hoepfner D, Seeber A, Loewith R, Movva NR, Gasser SM (2013). TORC2 signaling pathway guarantees genome stability in the face of DNA strand breaks. Mol Cell 51, 829–839.

Sikorski RS, Heiter P (1989). A system of shuttle vectors and yeast host strains designed for efficient manipulation of DNA in Saccharomyces cerevisiae. Genetics 122, 19–27.

Taulet N, Delorme-Walker VD, DerMardirossian C (2012). Reactive oxygen species regulate protrusion efficiency by controlling actin dynamics. PLoS One 7, e41342.

Vilella F, Herrero E, Torres J, de la Torre-Ruiz MA (2005). Pkc1 and the upstream elements of the cell integrity pathway in Saccharomyces cerevisiae, Rom2 and Mtl1, are required for cellular responses to oxidative stress. J Biol Chem 280, 9149–9159.

Yamane-Sando Y, Shimobayashi E, Shimobayashi M, Kozutsumi Y, Oka S, Takematsu H (2014). Fpk1/2 kinases regulate cellular sphingoid long-chain base abundance and alter cellular resistance to LCB elevation or depletion. Microbiologyopen 3, 196–212.